Application of the Karhunen-Loève Transform to the C5G7 benchmark in the Response Matrix Method

Richard L. Reed, Jeremy A. Roberts

Mechanical and Nuclear Engineering, Kansas State University, Manhattan, KS
rlreed@k-state.edu, jaroberts@k-state.edu

INTRODUCTION

Previous work used the Karhunen-Loève Transform (KLT) to create basis sets for representing the energy variable in the eigenvalue response matrix method (ERMM) and demonstrated the efficiency of such basis sets for 1-D problems.[?,?] The present work provides an extension of the KLT basis sets to the 2-D, C5G7 benchmark problem. ERMM solves the reactor eigenvalue equation,

$$\mathcal{T}\phi(\boldsymbol{\rho}) = \frac{1}{k}\mathcal{F}\phi(\boldsymbol{\rho}), \tag{1}$$

where $\boldsymbol{\rho}$ contains the relevant phase space (i.e., space, angle, and energy), by decomposing the domain into independent nodes linked through approximate boundary conditions that are based on truncated, orthogonal basis expansions. The success of ERMM in realistic applications is highly dependent on the selection of orthogonal bases in each phase space variable. Basis sets that capture high-fidelity transport solutions with low-order expansions are ideal. In what follows, ERMM and KLT basis are briefly reviewed, and their application to a modified C5G7 problem is presented.

METHODS

Overview of ERMM

Suppose the global problem of Eq. (**??**) is defined over a volume, V, which can be decomposed into N disjoint, nodal subvolumes, V_i, that satisfy $V = V_1 \bigcup V_2 \bigcup \ldots \bigcup V_N$. Then a local transport problem for the ith node is defined

$$\mathcal{T}\phi(\boldsymbol{\rho}_i) = \frac{1}{k}\mathcal{F}\phi(\boldsymbol{\rho}_i), \tag{2}$$

subject to the incident current boundary condition

$$J_-(\boldsymbol{\rho}_{is}) = J_-^{\text{global}}(\boldsymbol{\rho}_{is}), \tag{3}$$

where $J_-(\boldsymbol{\rho}_{is})$ is the incident angular current on surface s. To reduce the size of the problem space, the local boundary currents are represented as a truncated expansion in an orthogonal basis, $P_m(\boldsymbol{\rho}_{is})$, $m = 0, 1, \ldots$, defined over the surface phase space $\boldsymbol{\rho}_{is}$. By solving Eq. **??** subject to the mth order incident condition

$$J_-(\boldsymbol{\rho}_{is}) = P_m(\boldsymbol{\rho}_{is}) \tag{4}$$

on one surface, s, and vacuum elsewhere, a response function is defined as

$$r^{ms}_{im's'} = \int d\rho_{is'} P_{m'}(\boldsymbol{\rho}_{is'}) J_+(\boldsymbol{\rho}_{is'}), \tag{5}$$

where J^+ is the outgoing angular current. The response function $r^{ms}_{im's'}$ is the m'th order current response out of surface s' due to an mth order incident current on surface s.

By expressing the incident and outgoing currents, $J_\mp$, as truncated expansions in the basis, global neutron balance can be represented by the response matrix equation

$$\mathbf{MR}(k)\mathbf{J}_- = \lambda\mathbf{J}_-, \tag{6}$$

where $\mathbf{R}$ contains response functions, $\mathbf{J}_-$ contains the incident angular current expansion coefficients, $\mathbf{M}$ is a matrix that redirects outgoing currents as incident currents of neighbors, and λ is an eigenvalue that approaches unity as k approaches its correct value. The k-eigenvalue is computed iteratively by alternately solving for $\mathbf{J}_-$ and updating k based on balance.[?]

Expanding in Energy

The present work focused solely on expansion of the energy variable. Traditionally, RMMs have used a full multigroup representation of the energy variable, which is to say no truncation for the energy basis is used. Response matrix methods have been used successfully with a variety of energy group structures, ranging from three to 190 groups.[?,?,?]

In general, RRM is prohibitively expensive unless the problem space is greatly reduced by truncating the boundary conditions to each node. Thus, an effective basis set will permit the use of a low-order expansion without introducing a large error. Realistic problems require on the order of dozens of energy groups or more, and a basis that can capture many-group fidelity with many fewer energy degrees of freedom would be of substantial value to RMM.

Recent work investigated the use of discrete Legendre polynomials (DLP) and modified DLP (mDLP) for expansion in energy.[?] The mDLP basis modifies the DLP basis by superimposing a "shape" vector on each basis vector. The shape vector is chosen to be representative of the vector subject to expansion, i.e., the energy-dependent angular current. Previously, a spatially averaged energy spectrum from a representative lattice problem has been used with moderate success.[?]

The Karhunen-Loève Energy Basis

A more powerful approach (compared to mDLP) of incorporating physics into the basis functions is to use the Karhunen-Loève transform (KLT).[?] The central goal of KLT is to approximate a discrete or continuous function $f(x)$ as a truncated expansion in an orthogonal basis whose functions yield the best possible nth-order approximation in terms of least-squares error for all values of n by extracting information about the representative spectra in the problem space. In some applications, such as image compression, the function f is predetermined, e.g., a set of pixel values, while in other applications, such as reduced-order modeling, the function f is not known. While details of its use in these applications may differ, KLT is fundamentally related to the singular value decomposition (SVD).[?]

The implementation algorithm for computing the basis functions, $P^i_{\text{KLT}}(:)$, begins by forming the data matrix $\mathbf{D}$. Let the nth current vector be denoted by $\mathbf{d}_n$. These vectors, referred to as snapshots, are combined to form the matrix $\mathbf{D} \in \mathbb{R}^{G\times N}$, which is defined as $\mathbf{D} = [\mathbf{d}_1, \mathbf{d}_2, \ldots, \mathbf{d}_N]$,[?] where G is the number of energy groups and N is the total number of snapshots. Then the matrix $\mathbf{B} \in \mathbb{R}^{N\times N}$ is defined as

$$\mathbf{B} = \mathbf{D}^{\mathsf{T}}\mathbf{D}\,. \tag{7}$$

Next, find the eigenvectors corresponding to the largest eigenvalues of the matrix $\mathbf{B}$,

$$\mathbf{B} = \mathbf{Q}\mathbf{\Lambda}\mathbf{Q}^{-1}\,, \tag{8}$$

where $\mathbf{Q}$ from Eq. (**??**) is equal to $\mathbf{V}$ from the SVD of $\mathbf{D}$, and is thus the set of eigenvectors of $\mathbf{D}$. The eigenvectors $\mathbf{q}_j$ (columns of $\mathbf{Q}$ from Eq. (**??**)), are then multiplied by the data matrix to form the basis vectors $P^j_{KLT}(:)$, i.e.,

$$P^j_{KLT}(:) = \mathbf{D}\mathbf{q}_j\,, \tag{9}$$

which are subsequently orthonormalized. Then, an approximate representation of an arbitrary N-vector $\mathbf{f}$ in the basis is

$$\mathbf{f} \approx \sum_j a_j P^j_{KLT}(:) \quad \text{where} \quad a_j = \mathbf{f}^T P^j_{KLT}(:)\,. \tag{10}$$

Since KLT requires information about the solution *a priori*, small models that are similar to the test problem are developed to provide the necessary information. This work identifies how similar the small models need be to provide an adequate representation of the test problem. KLT snapshots are energy group-dependent flux or current vectors from several spatial cells within one or more representative models.

Test Problem

To test the application of KLT in 2-D space, the C5G7 benchmark problem was adapted for use. This benchmark consists of modeling a quarter core that has four, 17×17-pin assemblies.[?] The configuration is detailed in Fig. **??**. Each of the blocks in Fig. **??** represent either a fuel assembly or an equivalent area of moderator. Each pincell is broken up into a 7×7 Cartesian mesh. Thus, each pincell contained 49 spatial cells and provided 49 energy dependent snapshots of each type (scalar flux, partial current, etc.). The cladding for the pincells was homogenized into the fuel part of the pincell.

The standard C5G7 benchmark uses seven-group cross-sections, which precludes the need for an energy approximation. Thus, a cross section library was generated with SCALE 5.1 in the SCALE 44-group format.[?] All other aspects of the benchmark were unchanged.

For this test problem, the spatial and angular orders for the SERMENT[?] reference solution and the RMM solutions for each snapshot case were set to fourth order. It is assumed that the relative error of the snapshot cases is a function of the energy expansion alone since all other aspects of the problem are identical between the reference solution and each test case. It is impossible to be sure if this assumption is valid without computing the problem at better resolution.

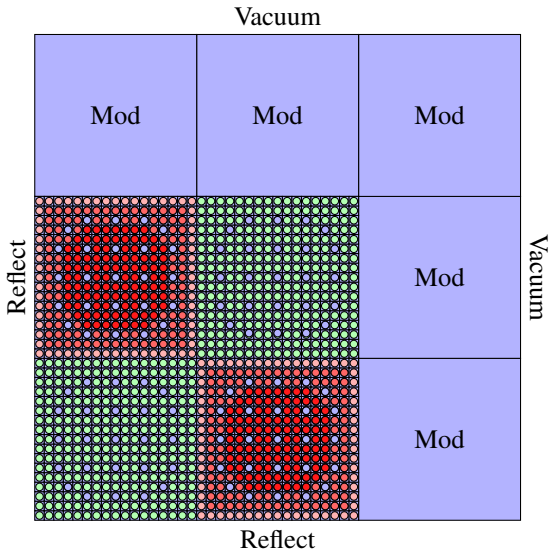

Fig. 1. Configuration for C5G7 benchmark. Each square represents the area of a 17×17 pin assembly

Generation of Snapshots

There are several models that are readily apparent choices to simplify the C5G7 benchmark for use in generating snapshots. The snapshots models for this test problem are summarized in Table **??**. The first model was to use snapshots from the test problem itself to gain an understanding of the best possible snapshots. However, the number of snapshots obtained for this model is prohibitively large, even after removing all duplicate snapshots by model symmetry, and thus unusable in the raw state. However, by spatially averaging the snapshots over a pincell, the number of snapshots is reduced by a factor of 49, and thus becomes a manageable set with which to create basis functions.

The Combined-Assemblies model was formed by taking snapshots from each assembly and combining the snapshots together. For this snapshot model, each assembly was modeled with reflective conditions on all sides. The next model was the Combined-Pins model, which derives snapshots from individual pincells for each fuel type. The pincell snapshots are combined with snapshots from junctions of pincells. These junctions are modeled as 2×2-pin assemblies with reflective conditions. There were a total of five different materials, thus ten unique junctions to model.

The next model was to create a small version of the C5G7 core, which has the same assembly configuration shown in Fig. **??**, but instead uses 8×8-pin assemblies.[?] An additional model arises from the small core model, which is to combine snapshots from each of the small assemblies. This is not expected to perform as well as the full-sized, combined-assembly model, but it will be quicker to create the snapshots, and thus the basis functions. A third model from the small core was to spatially average the snapshots over each pincell similarly to the spatially-reduced, full-core solution. The reduced, small-core model was used to approximate the non-spatially averaged, full-core model by comparing the reduced and non-reduced

TABLE I. Summary of snapshot models for C5G7 test Problem

Abbreviation	Model to generate snapshots
Reduced Full-Core	Spatially-averaged snapshots from whole core model (i.e., the test problem)
Combined-Assemblies	Snapshots from assemblies used in core configuration
Combined-Pins	Snapshots from pins used in core configuration combined with the pin junctions
Small-Core	Snapshots from the small core model
Small-Assemblies	Snapshots from the small assemblies used in the small core configuration
Reduced Small-Core	Spatially-averaged snapshots from the small core model
1-D Approximation	Snapshots from the 1-D approximation to the C5G7 benchmark

small-core models.

The final snapshot model for the C5G7 test problem is to create a similar 1-D model[?] with three sections: UO_2, MOX, and moderator. The model is comprised of 51 pins that are each of width 1.26 cm. This problem was created with a reflective boundary condition on the UO_2 side of the model and a vacuum boundary condition on the moderator side of the model.

In general, snapshot models should be computationally quick to solve, yet similar to the test problem. Timing studies provide little insight in this case because the snapshots are orders of magnitude quicker to generate than the response matrices. Furthermore, it is impossible to know *a priori* how many basis functions are required for accuracy before generating the response matrices.

RESULTS AND ANALYSIS

The goal of this work was to see how applicable the method of snapshots and the KLT was to 2-D problems. In the interest of time, the results for this section have been truncated to 10th order. The overarching goal of the work was to achieve sub-0.1% relative pin power errors while reducing the necessary energy degrees of freedom by an order of magnitude. As such, 10th order is sufficient to determine if KLT can reach the goal in a 2-D problem-space. As mentioned previously, we assume any changes in the solution observed when using various energy bases is assumed to be a function of the energy basis alone.

Each curve shown in this section except for 'DLP' and 'mDLP' was generated using the KLT basis with distinct snapshot data. The mDLP results represent the best case previously observed.[?] Figure **??** presents the results from using snapshots of only the scalar flux ϕ in the KLT basis generation in order to approximate the nodal fission densities. Many of the snapshot models fall short of the goal of sub 0.1% relative error in the first 10 degrees of freedom, but some snapshot models perform encouragingly well. The Small-Core performs the best at 9th order, but the Combined-Pins model performs encouragingly well despite its simplicity. Further, the Small-Core models performs similarly to the Reduced Small-Core, thus we may assume that the Reduced Full-Core model provides a close approximation to the Full-Core results.

In general, the results are improved by including snapshots of the partial current J for basis generation as shown in Fig. **??**. The Combined-Pins model performs quite well comparatively, and achieves the goal by 9th order. However, it is unknown if the relative error will remain below the goal at higher orders

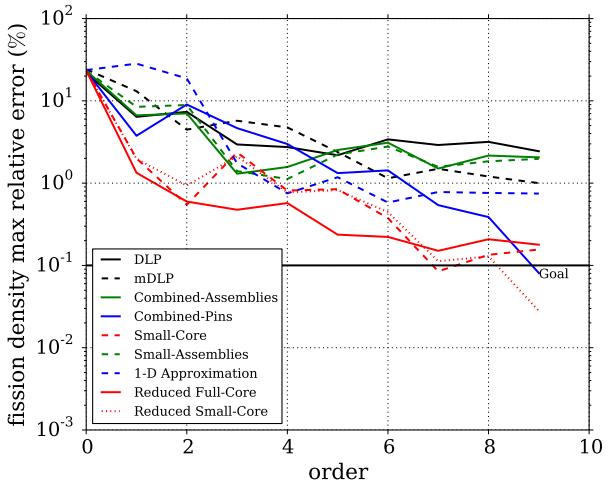

Fig. 2. Relative error in fission density for 44-group, C5G7 test problem using snapshot of only ϕ.

without running additional calculations. Further, the Small-Core results are omitted because the number of snapshots was too high to apply KLT without averaging, thus we must take the Reduced Small-Core model as an approximation for the performance of the Small-Core model.

Many of the same trends are observed for pin-power errors as shown in Fig. **??** and **??**. The former uses snapshots of only ϕ, while the latter also includes snapshots of J. Since pin powers are a local quantity, it was expected (and observed) that the errors are larger than for the more global nodal fission densities.

CONCLUSION

For 2-D problems, many KLT basis outperform the mDLP and DLP bases for ERMM energy expansions because the KLT maximizes the information contained in low-order expansions. In general, the results are improved by including the partial current in generation of snapshots as opposed to using only the scalar flux snapshots.

An effective snapshot model is one that can capture the relevant physics of the problem while being computationally cheap. The Combined-Pins model performed quite well despite its simplicity likely because information about each fuel type as well as the junction between materials were used in the construction.

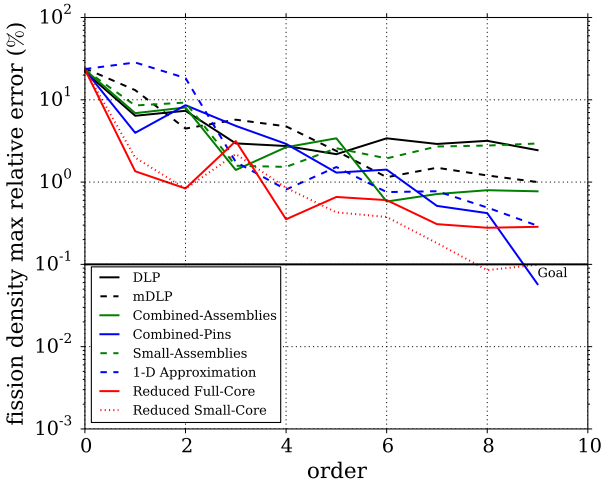

Fig. 3. Relative error in fission density for 44-group, C5G7 test problem using snapshot of ϕ, J_{up}, and J_{down}.

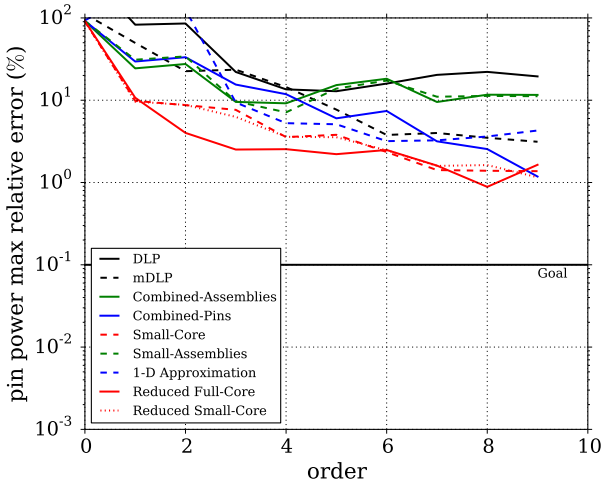

Fig. 4. Relative error in pin power for 44-group, C5G7 test problem using snapshot of only ϕ.

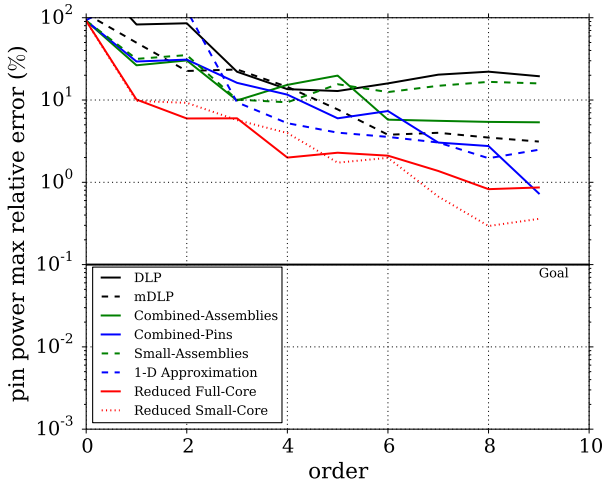

Fig. 5. Relative error in pin power for 44-group, C5G7 test problem using snapshot of both ϕ, J_{up}, and J_{down}.

It appears that for heterogeneous problems such as the C5G7 benchmark, a basis expansion in the energy variable requires more degrees of freedom to reach the goal of sub-0.1% relative error as compared to the 1D problems previously explored.[?,?] Future work in this area would entail expanding this application to additional group structures to ensure the results are not group dependent. Additionally, it would be interesting to explore applications of the KLT to expansion in other phase space variables.

ACKNOWLEDGEMENTS

The work of the first author was supported by the Kansas State University Nuclear Research Fellowship Program, generously sponsored by the U.S. Nuclear Regulatory Commission (Grant NRC-HQ-84-14-G-0033).